Electronic Supplementary Material (ESI) for New Journal of Chemistry.

Mechanistic Insights of Allylic Oxidation of Aliphatic Compound by Tetraamido Iron(V) Species: A C-H vs O-H Bond Activation

Monika and Azaj Ansari*

Department of Chemistry, Central University of Haryana, Mahendergarh 123031, India.

Email: ajaz.alam2@gmail.com

Table S1. B3LYP-D2/B3LYP/wB97XD computed relatives energies of *Pathway a* and *Pathway b*.

Pathway a				Pathway b			
	B3LYP-D2	B3LYP	wB97XD		B3LYP-D2	B3LYP	wB97XD
^{4}I	5.2	5.5	24.9	^{4}I	5.2	5.5	24.9
^{2}I	0	0	0	^{2}I	0	0	0
^{4}ts$_a$-1	71.5	85.8	158.5	^{4}ts$_b$-1	84.5	108.4	137.4
^{2}ts$_a$-1	64.9	85.0	120.8	^{2}ts$_b$-1	60.7	125.7	102.9
^{6}Int$_a$	55.0	54.3	47.1	^{6}Int	-49.6	-53.3	-60.1
^{4}Int$_a$	30.9	30.9	55.2	^{4}Int	-73.7	-76.6	-51.9
^{2}Int$_a$	112.9	114.6	112.1	^{2}Int	8.3	6.96	4.8
^{6}ts$_a$-2$_{hs}$	82.0	103.5	124.4	^{6}ts$_b$-2$_{hs}$	-73.6	-14.5	12.5
^{4}ts$_a$-2$_{hs}$	53.7	82.6	59.6	^{4}ts$_b$-2$_{hs}$	-	-	-
^{4}ts$_a$-2$_{is}$	55.6	79.1	83.1	^{4}ts$_b$-2$_{is}$	-	-70.3	-59.9
^{2}ts$_a$-2$_{is}$	68.8	66.0	43.2	^{2}ts$_b$-2$_{is}$	-39.1	-38.0	-
^{2}ts$_a$-2$_{ls}$	64.2	84.9	96.2	^{2}ts$_b$-2$_{ls}$	-	-3.8	-
^{6}P	-196.4	-101.3	-228.36	^{6}P	-196.44	-101.32	-228.36
^{4}P	-285.3	-305.7	-316.12	^{4}P	-285.32	-305.79	-316.12
^{2}P	-285.6	-224.9	-221.78	^{2}P	-285.69	-224.91	-221.78

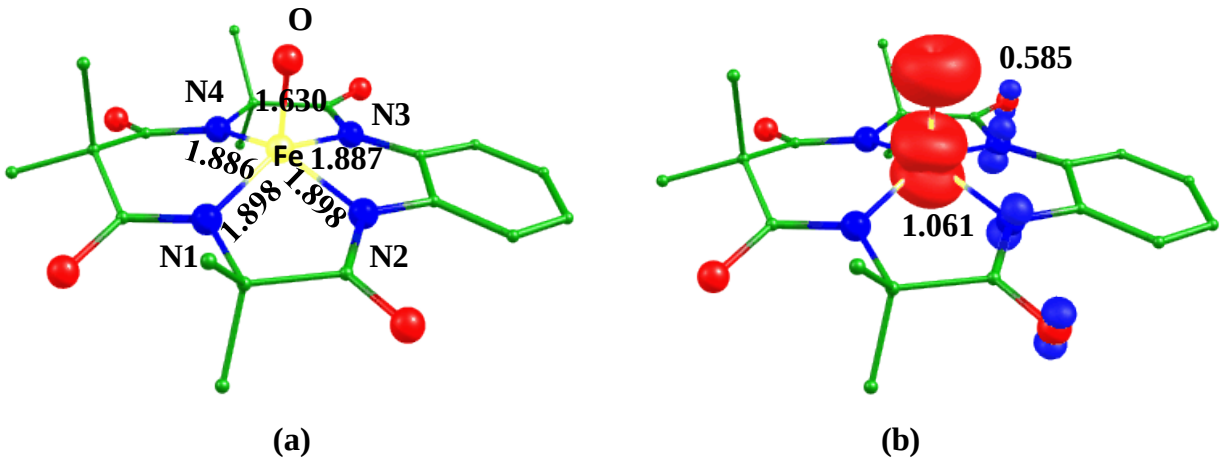

Fig. S1. B3LYP-D2 a) optimized structure (bond lengths in Å) of low spin and its b) spin density plot

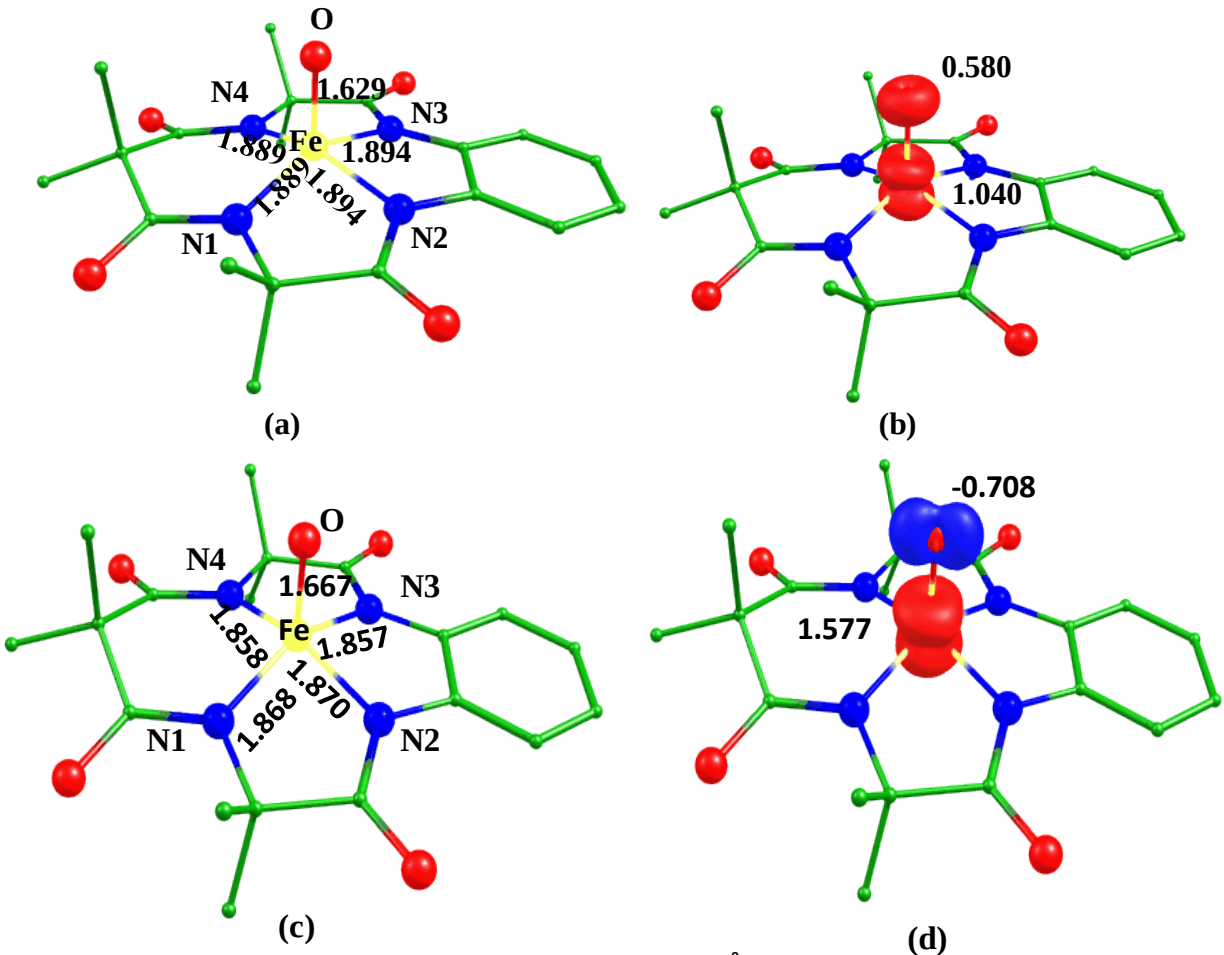

Fig. S2. a) B3LYP optimized structure (bond lengths in Å) of low spin and its b) spin density plot, c) wB97XD optimized structure of low spin and its d) spin density plot.

Table S2. B3LYP-D2 computed structural parameters of the $[Fe^{V}(TAML)O]^{-}$ species, intermediates transition states and Product of *Pathway a*.

	Bond lengths (Å)										Bond angle (°)					
	Fe-N1	Fe-N2	Fe-N3	Fe-N4	Fe-O1	O1-H1	O1-H2	H1-O2	H2-C1	C1-O2	Fe-O1-H1	Fe-O1-H2	O1-H1-O2	O1-H2-C1	N1-Fe-N3	N2-Fe-N4
^{4}I	1.914	1.914	1.878	1.878	1.664	-	-	-	-	-	-	-	-	-	155.7	155.8
^{2}I	1.898	1.898	1.887	1.886 1.87[1]	1.630 1.58[1]	-	-	-	-	-	-	-	-	-	152.2	152.1
^{4}ts$_{a}$-1	1.892	1.882	1.871	1.875	1.752	1.067	-	1.387		1.423	119.0		169.6		153.8	156.9
^{2}ts$_{a}$-1	1.894	1.897	1.874	1.872	1.737	1.077	-	1.397		1.435	109.0		169.7		156.9	152.0
^{6}Int$_{a}$	1.911	1.919	1.889	1.905	1.906	154.7	-	-	-	-	-	-	-	-	154.7	150.3
^{4}Int$_{a}$	1.877	1.877	1.879	1.879	1.803	0.982	-	-	-	-	-	-	-	-	155.0	155.0
^{2} Int$_{a}$	1.932	1.834	1.910	1.830	1.760	161.5	-	-	-	-	-	-	-	-	161.5	143.6
^{6}ts$_{a}$-$_{hs}$	1.884	1.912	1.875	1.877	2.010	-	1.297		1.327	-	-	115.9	-	173.8	160.4	153.1
^{4}ts$_{a}$-$_{hs}$	1.901	1.904	1.887	1.881	1.974	-	1.470		1.226	-	-	129.7	-	170.7	155.6	155.9
^{4}ts$_{a}$-2$_{is}$	1.887	1.898	1.883	1.890	1.886	-	1.598		1.174	-	-	130.5	-	166.7	156.2	153.9
^{2}ts$_{a}$-2$_{is}$	1.903	1.911	1.883	1.889	1.956	-	1.276		1.335	-	-	132.8	-	174.9	156.9	155.1
^{2}ts$_{a}$-2$_{ls}$	1.877	1.878	1.880	1.870	1.848	-	1.457		1.224	-	-	131.8	-	173.3	160.2	155.7
^{6}P	1.984	1.984	1.924	1.924	-	-	-	-	-	-	-	-	-	-	159.7	159.7
^{4}P	1.864	1.867	1.868	1.864	-	-	-	-	-	-	-	-	-	-	171.9	171.9
^{2}P	1.851	1.872	1.853	1.865	-	-	-	-	-	-	-	-	-	-	170.9	171.2

Table S3. B3LYP computed structural parameters of the $[Fe^{V}(TAML)O]^{-}$ species, intermediates, transition states and Product of *Pathway a*.

	Bond lengths (Å)										Bond angle (°)					
	Fe-N1	Fe-N2	Fe-N3	Fe-N4	Fe-O1	O1-H1	O1-H2	H1-O2	H2-C1	C1-O2	Fe-O1-H1	Fe-O1-H2	O1-H1-O2	O1-H2-C1	N1-Fe-N3	N2-Fe-N4
^{4}I	1.880	1.880	1.910	1.910	1.665	-	-	-	-	-	-	-	-	-	156.1	156.1
^{2}I	1.889	1.889	1.894	1.894	1.629	-	-	-	-	-	-	-	-	-	152.3	152.3
$^{4}ts_{a}$-1	1.897	1.902	1.878	1.878	1.720	1.142	-	1.289	-	1.443	117.2	-	174.2	-	154.2	154.4
$^{2}ts_{a}$-1	1.872	1.897	1.895	1.881	1.725	1.116	-	1.326	-	1.430	111.4	-	171.9	-	156.0	152.4
$^{6}Int_{a}$	1.892	1.908	1.910	1.918	1.910	0.979	-	-	-	-	-	-	-	-	154.4	150.3
$^{4}Int_{a}$	1.881	1.881	1.879	1.879	1.806	0.981	-	-	-	-	-	-	-	-	154.7	154.7
^{2} Int_{a}							-	-	-	-	-	-	-	-		
$^{6}ts_{a\text{-}hs}$	1.920	1.882	1.887	1.890	2.020	-	1.277	-	1.358	-	-	126.6	-	174.6	158.9	151.5
$^{4}ts_{a\text{-}hs}$	1.887	1.901	1.904	1.890	1.994	-	1.471	-	1.238	-	-	141.3	-	175.7	154.4	155.5
$^{4}ts_{a}$-2_{is}	1.889	1.895	1.885	1.898	1.911	-	1.549	-	1.200	-	-	141.4	-	172.6	156.3	152.7
$^{2}ts_{a}$-2_{is}	1.891	1.892	1.908	1.909	1.966	-	1.307	-	1.327	-	-	140.7	-	175.0	155.3	154.8
$^{2}ts_{a}$-2_{ls}	1.874	1.877	1.886	1.876	1.867	-	1.432	-	1.248	-	-	141.7	-	173.2	159.8	154.1
^{6}P	1.978	1.978	1.909	1.909	-	-	-	-	-	-	-	-	-	-	166.6	166.6
^{4}P	1.863	1.863	1.870	1.870	-	-	-	-	-	-	-	-	-	-	172.0	172.0
^{2}P	1.858	1.870	1.852	1.861	-	-	-	-	-	-	-	-	-	-	171.3	171.3

Table S4. wB97XD computed structural parameters of the $[Fe^{V}(TAML)O]^{-}$ species, intermediates, transition states and Product of *Pathway a*.

	Bond lengths (Å)										Bond angle (°)					
	Fe-N1	Fe-N2	Fe-N3	Fe-N4	Fe-O1	O1-H1	O1-H2	H1-O2	H2-C1	C1-O2	Fe-O1-H1	Fe-O1-H2	O1-H1-O2	O1-H2-C1	N1-Fe-N3	N2-Fe-N4
^{4}I	1.876	1.877	1.883	1.882	1.638	-	-	-	-	-	-	-	-	-	153.9	153.9
^{2}I	1.868	1.870	1.857	1.858	1.667	-	-	-	-	-	-	-	-	-	152.9	153.2
^{4}ts$_{a}$-1	1.860	1.861	1.857	1.870	1.742	1.098	-	1.275	-	1.423	118.7	-	167.1	-	159.0	153.7
^{2}ts$_{a}$-1	1.854	1.868	1.871	1.861	1.760	1.139	-	1.203	-	1.439	119.2	-	119.2	-	153.9	154.9
^{6}Int$_{a}$	1.875	1.890	1.891	1.899	1.889	0.972	-	-	-	-	-	-	-	-	154.6	150.5
^{4}Int$_{a}$	1.867	1.865	1.859	1.859	1.784	0.975	-	-	-	-	-	-	-	-	155.5	155.5
^{2} Int$_{a}$	1.903	1.804	1.913	1.810	1.735	0.977	-	-	-	-	-	-	-	-	163.7	1.810
^{6}ts$_{a\text{-}hs}$	1.872	1.880	1.864	1.844	2.017	-	1.241	-	1.371	-	-	116.2	-	172.2	157.8	156.7
^{4}ts$_{a\text{-}hs}$	1.904	1.890	1.887	1.901	1.994	-	1.471	-	1.238	-	-	141.3	-	175.8	154.4	155.5
^{4}ts$_{a}$-2$_{is}$	1.885	1.893	1.902	1.877	1.942	-	1.417	-	1.245	-	-	129.3	-	171.2	155.5	155.5
^{2}ts$_{a}$-2$_{is}$	1.909	1.891	1.892	1.908	1.966	-	1.307	-	1.327	-	-	140.7	-	175.0	155.4	154.8
^{2}ts$_{a}$-2$_{ls}$	1.900	1.907	1.874	1.879	1.971	-	1.226	-	1.379	-	-	130.9	-	172.4	156.4	154.9
^{6}P	1.959	1.959	1.908	1.908	-	-	-	-	-	-	-	-	-	-	162.3	162.3
^{4}P	1.849	1.858	1.858	1.858	-	-	-	-	-	-	-	-	-	-	172.1	172.1
^{2}P	1.831	1.852	1.833	1.863	-	-	-	-	-	-	-	-	-	-	172.0	172.2

Table S5. B3LYP-D2 computed spin density values of the $[Fe^{V}(TAML)O]^{-}$ species, intermediates, transition states and Product of *Pathway a*.

	Fe1	O1	H1	H2	O2	C1
^{4}I	1.279	0.757	-	-	-	-
^{2}I	1.061	0.585	-	-	-	-
$^{4}ts_{a}$-1	1.607	0.290	-0.017	-	0.519	-
$^{2}ts_{a}$-1	1.690	0.139	0.012	-	-0.447	-
$^{6}Int_{a}$	3.202	0.381	0.005	-	-	-
$^{4}Int_{a}$	1.788	0.036	0.010	-	-	-
$^{2}Int_{a}$	0	0	0	-	-	-
$^{6}ts_{a}$-2_{hs}	3.173	0.216	-	0.109	0.557	0.141
$^{4}ts_{a}$-2_{hs}	3.143	0.201	-	-0.119	-0.698	0.010
$^{4}ts_{a}$-2_{is}	2.319	0.038	-	0.110	0.795	-0.031
$^{2}ts_{a}$-2_{is}	2.468	0.051	-	-0.108	-0.625	-0.095
$^{2}ts_{a}$-2_{ls}	0.513	0.026	-	0.120	0.717	-0.016
^{6}P	3.914	-	-	-	-	-
^{4}P	2.663	-	-	-	-	-
^{2}P	1.187	-	-	-	-	-

Table S6. B3LYP computed spin density values of the $[Fe^{V}(TAML)O]^{-}$ species, intermediates , transition states and product of *Pathway a*.

	Fe1	O1	H1	H2	O2	C1
^{4}I	1.274	0.766	-	-	-	-
^{2}I	1.040	0.580	-	-	-	-
$^{4}ts_{a}$-1	1.649	0.251	0.251	-	0.419	-
$^{2}ts_{a}$-1	1.653	0.153	0.012	-	-0.382	-
$^{6}Int_{a}$	3.206	0.381	0.004	-	-	-
$^{4}Int_{a}$	1.804	0.037	0.009	-	-	-
$^{2}Int_{a}$	0	0	0	-	-	-
$^{6}ts_{a}$-2_{hs}	3.217	0.195	-	0.195	0.583	0.151
$^{4}ts_{a}$-2_{hs}	3.154	0.197	-	-0.123	-0.688	0.004
$^{4}ts_{a}$-2_{is}	2.358	0.026	-	0.116	0.757	-0.028
$^{2}ts_{a}$-2_{is}	2.450	0.062	-	-0.115	-0.614	-0.077
$^{2}ts_{a}$-2_{ls}	-0.003	-0.050	-	0.166	-0.031	0.084
^{6}P	3.921	-	-	-	-	-
^{4}P	2.664	-	-	-	-	-
^{2}P	1.228	-	-	-	-	-

Table S7. wB97XD computed spin density values of the $[Fe^{V}(TAML)O]^{-}$ species and their intermediates and transition states and product of *Pathway a*.

	Fe1	O1	H1	H2	O2	C1
^{4}I	2.312	0.645	-	-	-	-
^{2}I	1.577	-0.708	-	-	-	-
$^{4}ts_{a}$-1	1.500	0.414	-0.033	-	0.496	-
$^{2}ts_{a}$-1	1.866	-0.433	0.052	-	-0.531	-
$^{6}Int_{a}$	3.273	0.381	0.003	-	-	-
$^{4}Int_{a}$	1.804	0.014	0.009	-	-	-
$^{2}Int_{a}$	0.805	-0.601	0.393	-	-	-
$^{6}ts_{a}$-2_{hs}	3.211	0.222	-	0.101	0.560	0.178
$^{4}ts_{a}$-2_{hs}	3.154	0.197	-	-0.123	-0.688	0.004
$^{4}ts_{a}$-2_{is}	2.618	0.124	-	0.108	0.714	0.023
$^{2}ts_{a}$-2_{is}	2.451	0.062	-	0.008	-0.614	-0.077
$^{2}ts_{a}$-2_{ls}	2.628	0.067	-	-0.109	-0.584	-0.137
^{6}P	3.996	-	-	-	-	-
^{4}P	2.744	-	-	-	-	-
^{2}P	0.990	-	-	-	-	-

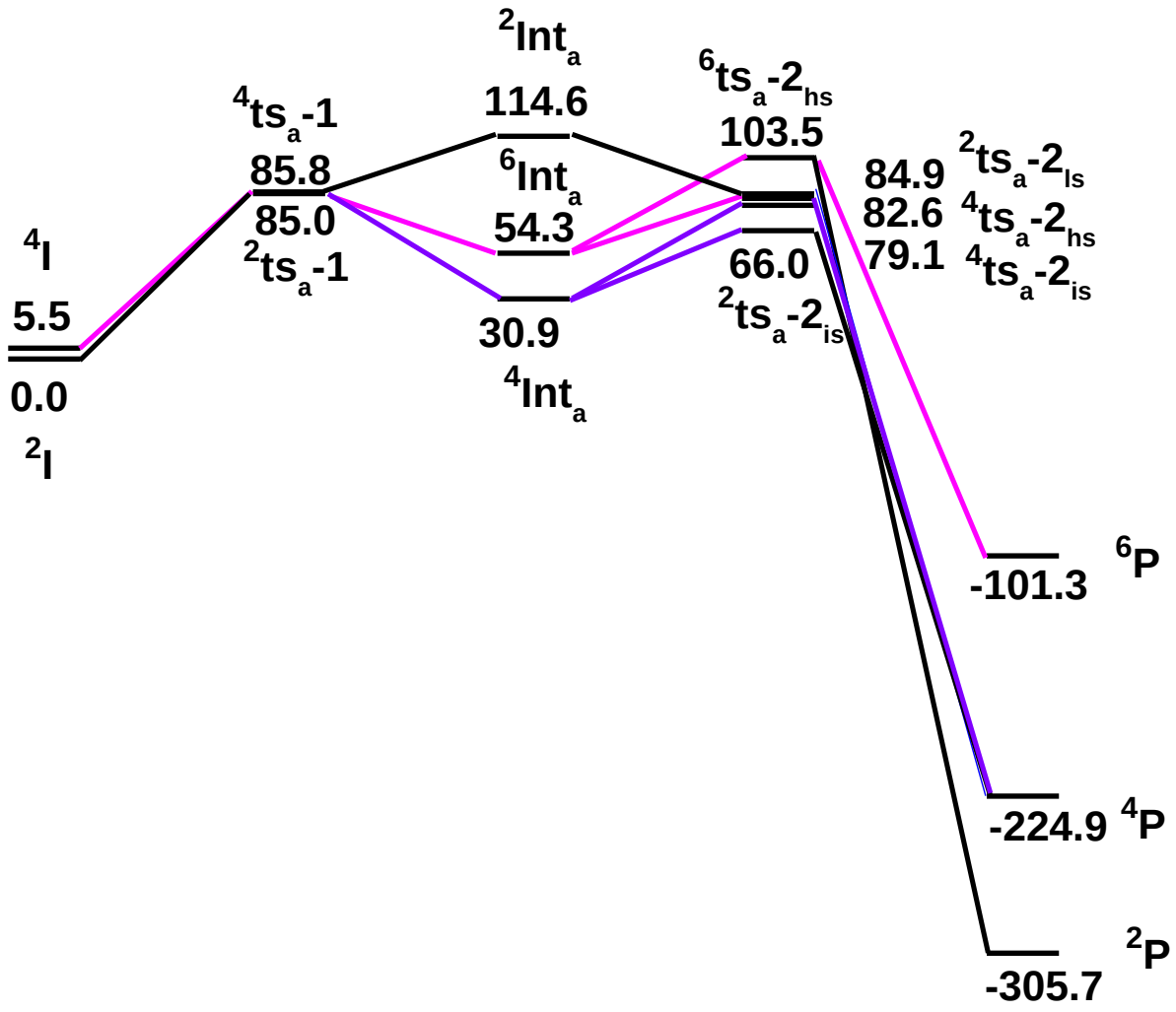

Fig. S3. B3LYP computed energy surface for the formation of cyclohex-2-enone from cyclohex-2-enol *via* O-H bond activation (***pathway a***) by Fe^{V}=O species (ΔG in $kJmol^{-1}$).

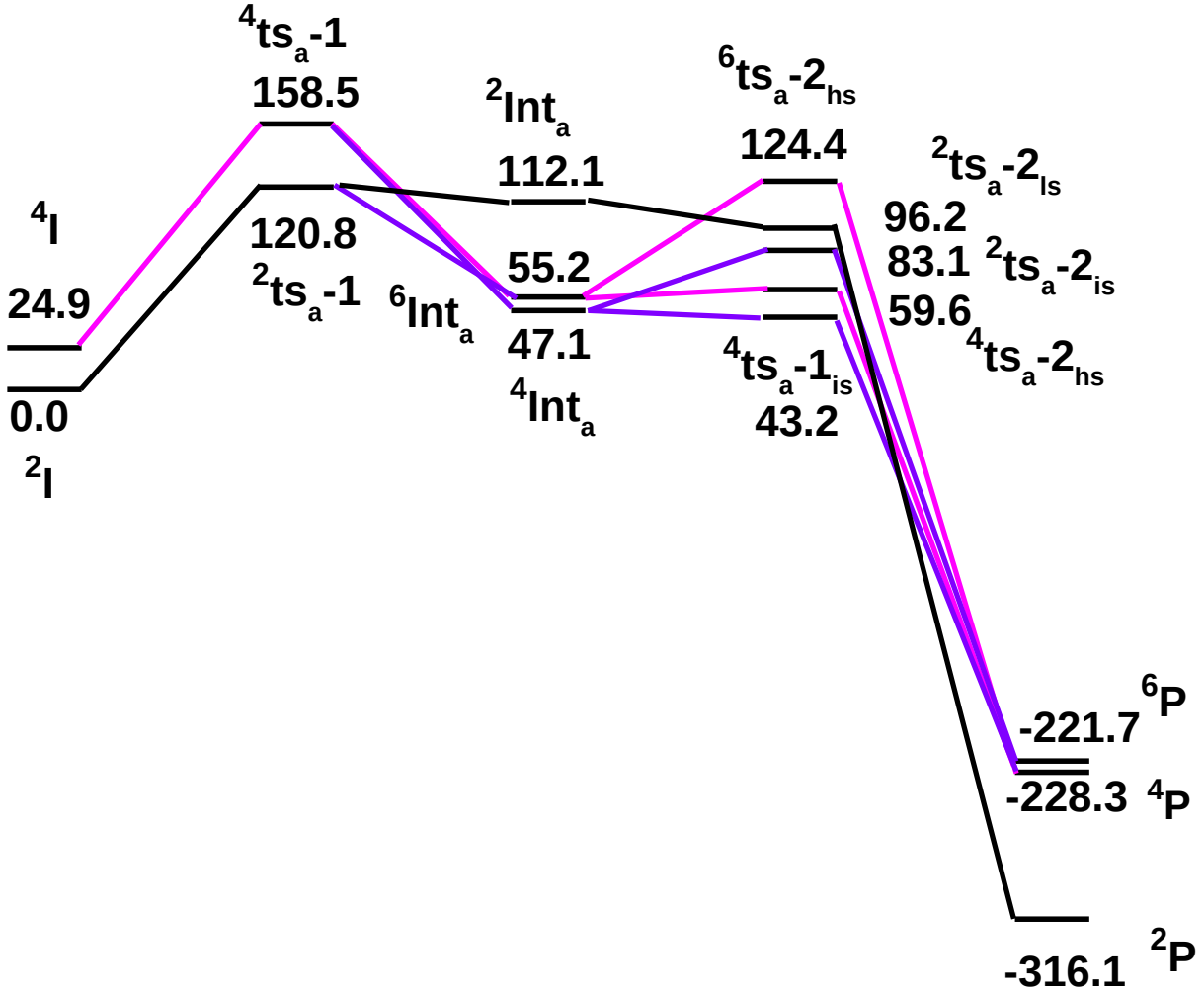

Fig. S4. wB97XD computed energy surface for the formation of cyclohex-2-enone from cyclohex-2-enol *via* O-H bond activation (***pathway a***) by Fe^{V}=O species (ΔG in $kJmol^{-1}$).

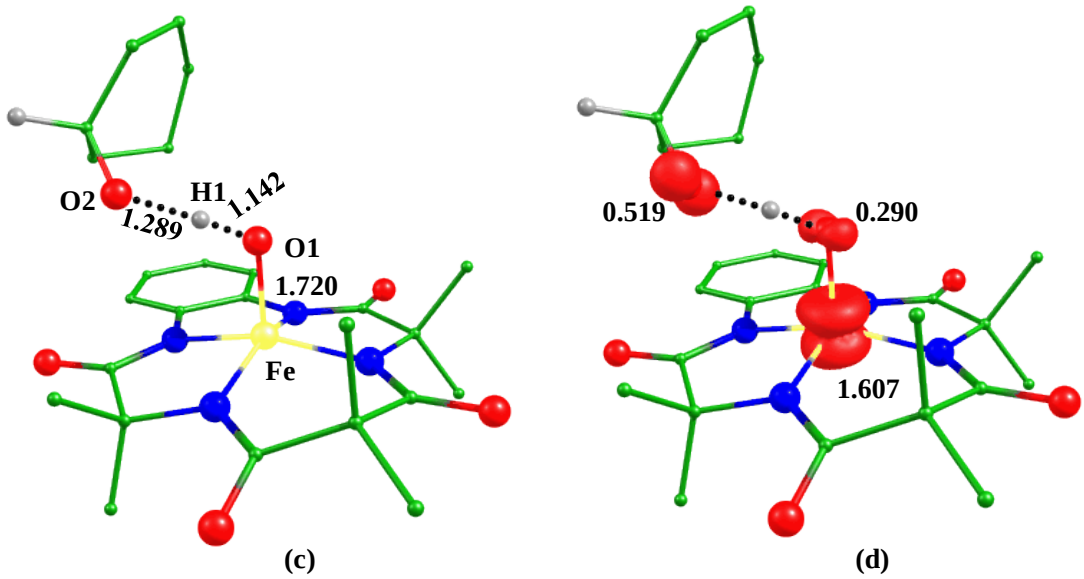

Fig. S5. B3LYP-D2 a) optimized structure (bond length in Å) and b) its spin density plot of the transition state $^{4}ts_{a}$-1.

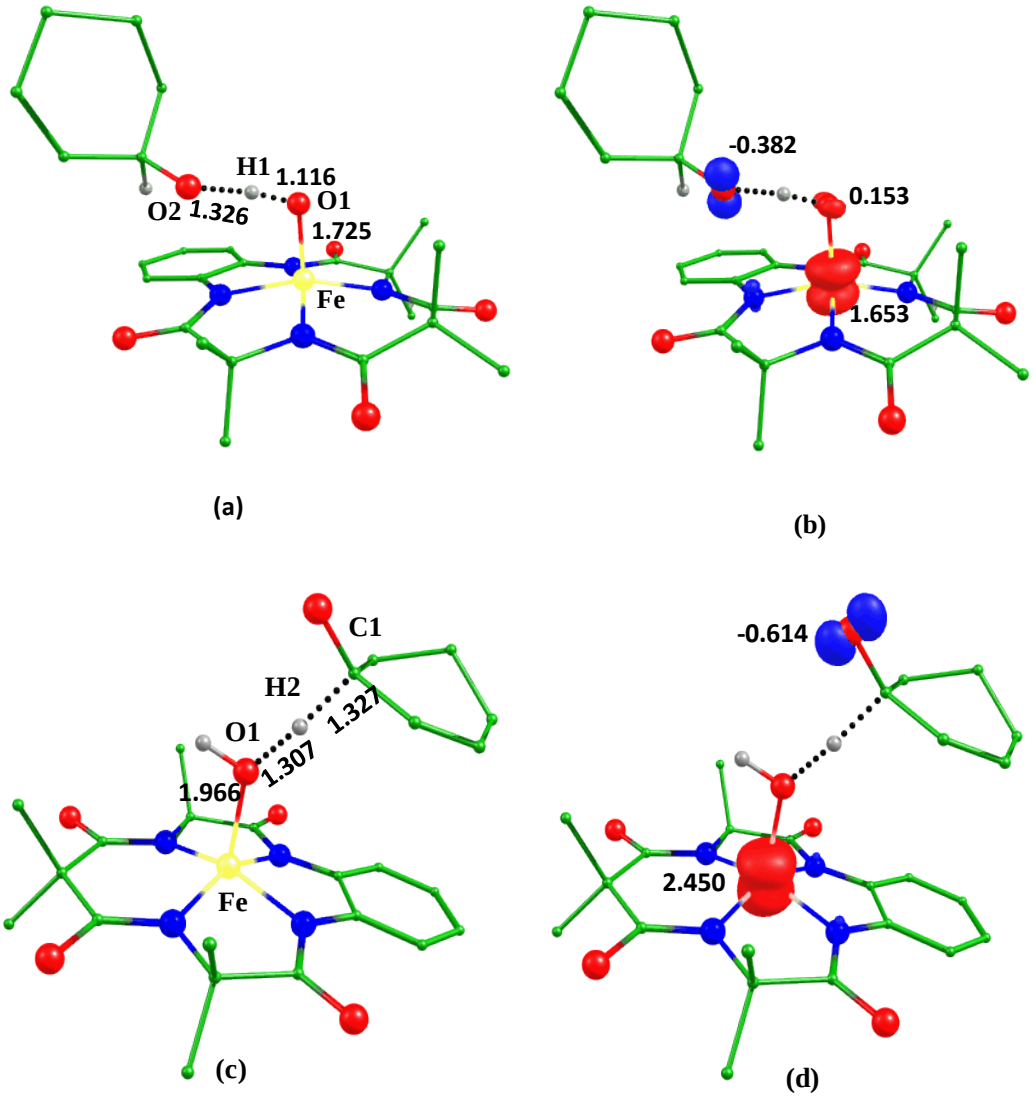

Fig. S6. B3LYP a) optimized structure (bond length in Å) and b) its spin density plot of the transition state $^{2}ts_{a}$-1, c) optimized structure and d) its spin density plot of the transition state $^{2}ts_{a}$-2_{is}.

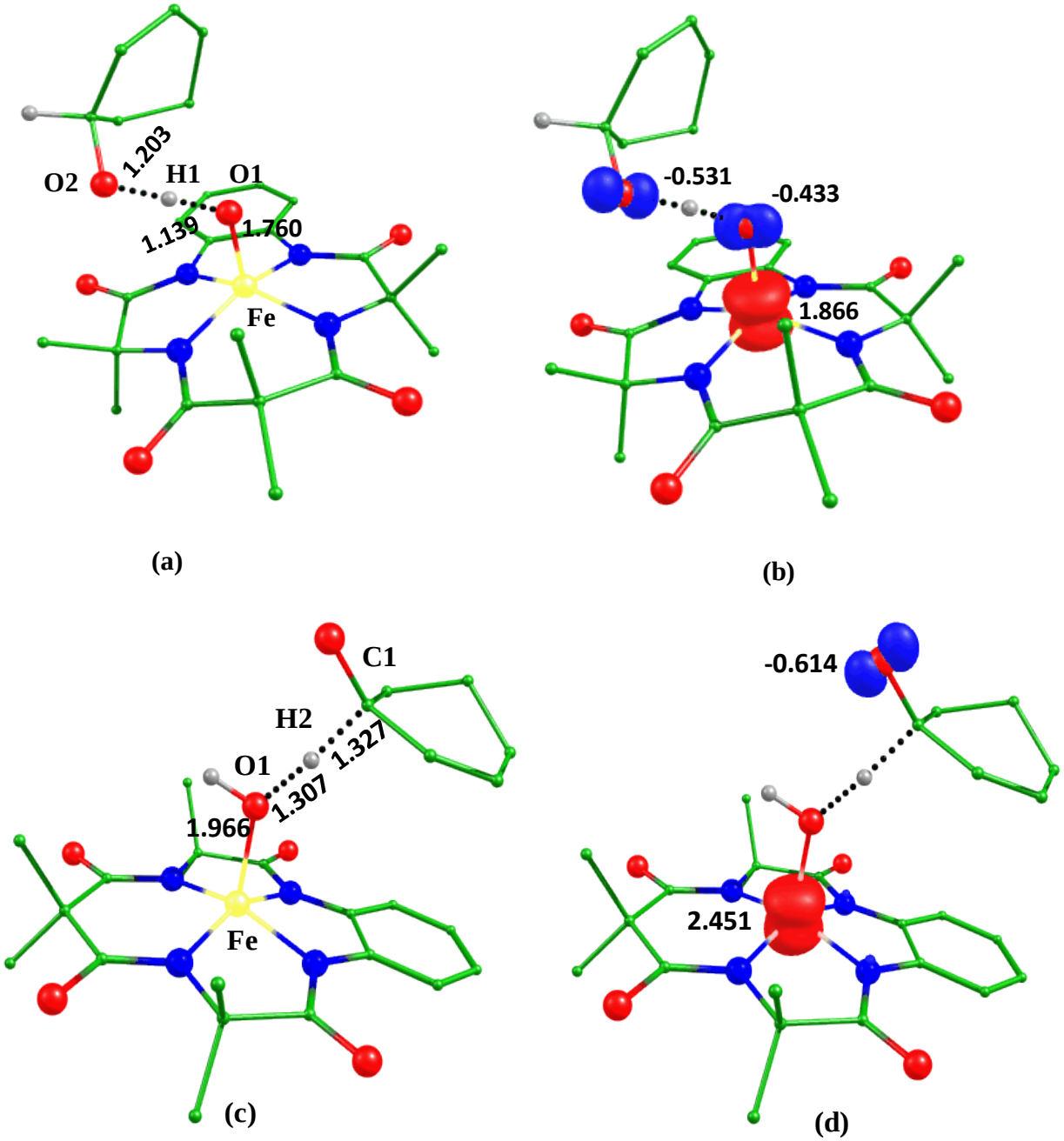

Fig. S7. wB97XD a) optimized structure (bond length in Å) and b) its spin density plot of the transition state $^{2}ts_{a}$-1, c) optimized structure and d) its spin density plot of the transition state $^{2}ts_{a}$-2_{is}.

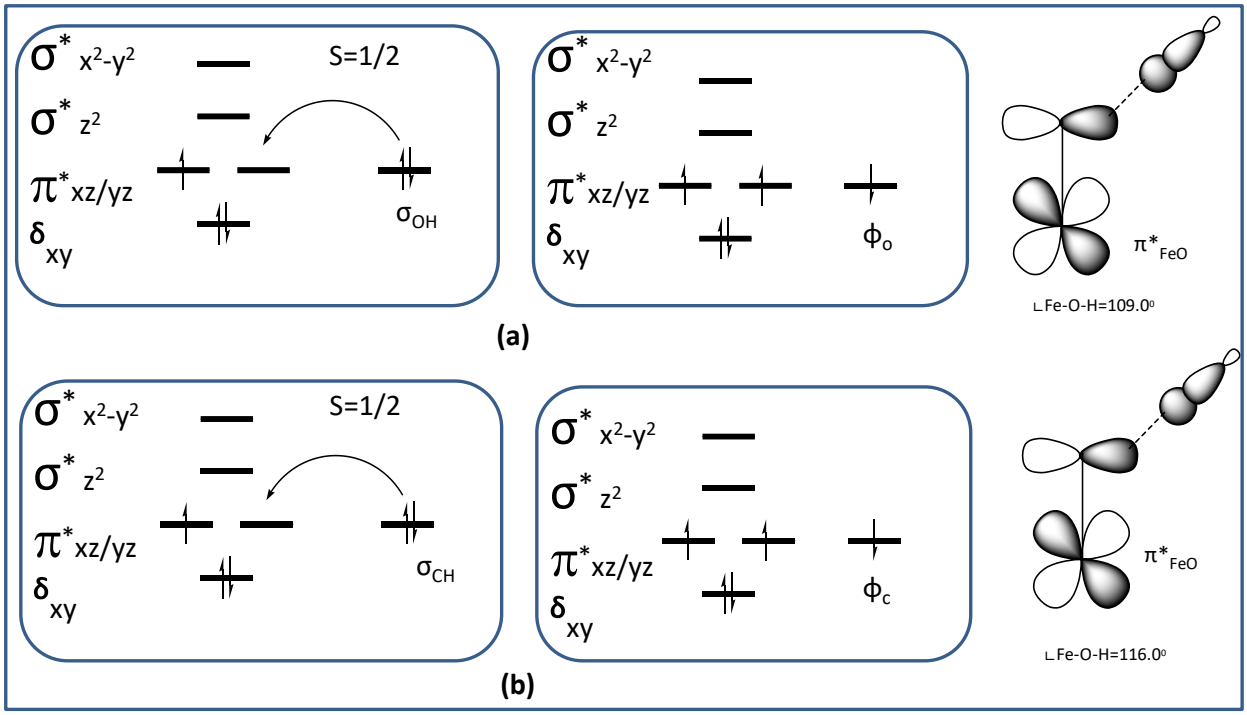

Scheme S1. Orbital occupancy diagrams for the H-abstraction of (a) ^2ts_a-1 and (b) ^2ts_b-1.

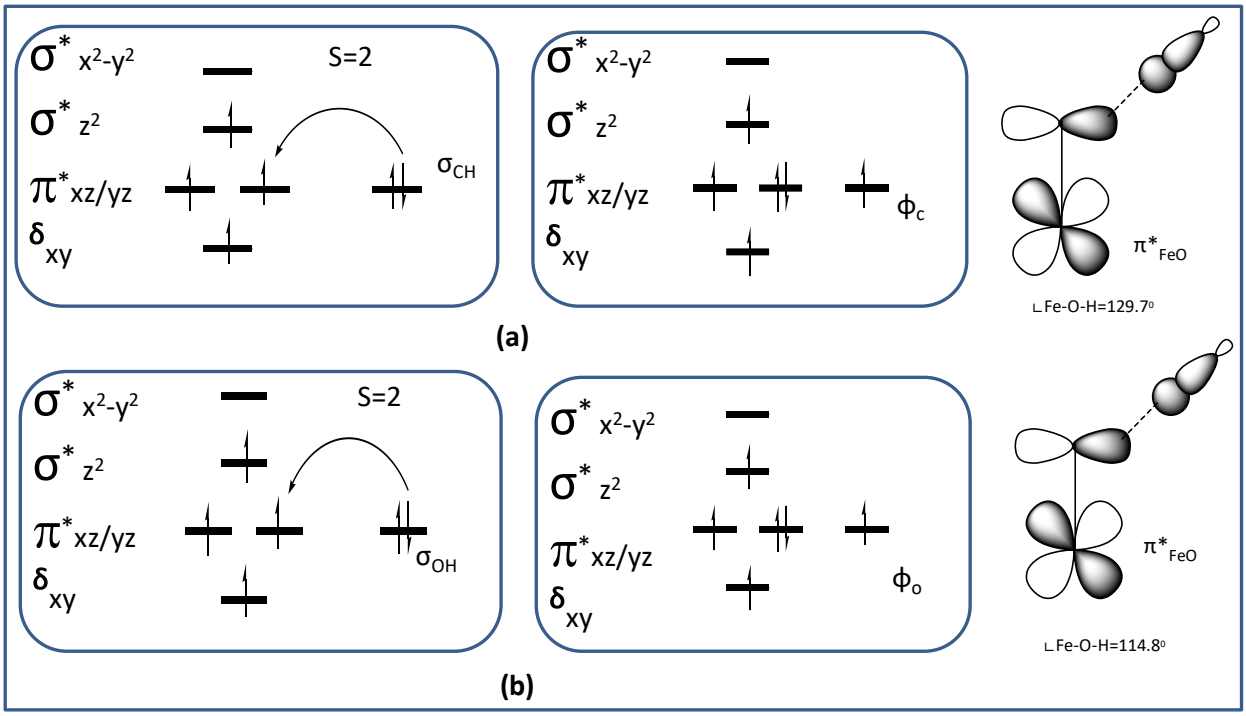

Scheme S2. Orbital occupancy diagrams for the H-abstraction of (a) ^{4}**ts$_{a}$-2$_{hs}$** and (b) ^{6}**ts$_{b}$-2$_{hs}$.**

Table S8. B3LYP-D2/B3LYP/wB97XD computed structural parameters of the transition states of *Pathway b*.

	Bond lengths (Å)										Bond angle (°)					
	Fe-N1	Fe-N2	Fe-N3	Fe-N4	Fe-O1	O1-H1	O1-H2	H1-O2	H2-C1	C1-O2	Fe-O1-H2	Fe-O1-H1	O1-H2-C1	O1-H1-O2	N1-Fe-N3	N2-Fe-N4
B3LYP-D2																
$^{4}ts_{b}$-1	1.920	1.915	1.890	1.893	1.740	-	1.371	-	1.199	1.445	134.9	-	174.2	-	152.3	153.5
$^{2}ts_{b}$-1	1.877	1.894	1.873	1.892	1.684	-	1.470	-	1.178	1.441	116.0	-	161.3	-	150.8	154.1
$^{6}ts_{b-hs}$	2.027	2.035	1.973	1.963	1.993	1.807	-	1.009	-	1.343	-	114.8	-	116.7	144.4	145.0
$^{2}ts_{b}$-2_{is}	1.876	1.879	1.891	1.879	1.844	2.220	-	0.983	-	1.377	-	103.5	-	105.6	155.8	158.4
B3LYP																
$^{4}ts_{b}$-1	1.910	1.901	1.904	1.914	1.777	-	1.266	-	1.257	1.444	160.3	-	160.3	-	151.6	152.2
$^{2}ts_{b}$-1	1.874	1.883	1.883	1.883	1.737	-	1.336	-	1.242	1.442	117.5	-	152.3	-	153.6	153.0
$^{6}ts_{b-hs}$	2.035	1.972	1.962	1.972	1.993	1.807	-	1.008	-	1.343	-	114.8	-	116.7	145.0	144.3
$^{2}ts_{b-is}$	1.891	1.893	1.898	1.898	2.138	1.554	-	1.058	-	1.342	-	120.8	-	125.3	160.3	158.1
$^{2}ts_{b}$-2_{is}	1.879	1.891	1.878	1.876	1.843	2.220	-	0.982	-	1.377	-	103.5	-	105.5	155.7	158.4
$^{2}ts_{b}$-2_{ls}	1.880	1.884	1.896	1.886	1.882	2.317	-	0.981	-	1.373	-	109.7	-	99.0	158.1	154.5
wB97XD																
$^{4}ts_{b}$-1	1.880	1.895	1.893	1.874	1.739	-	1.452	-	1.162	1.439	134.2	-	174.6	-	152.2	154.2
$^{2}ts_{b}$-1	1.874	1.883	1.883	1.894	1.737	-	1.336	-	1.242	1.442	117.5	-	152.3	-	153.6	153.0
$^{6}ts_{b-hs}$	2.006	1.964	1.952	1.997	2.008	1.770	-	1.010	-	1.320	-	111.5	-	116.2	147.0	145.6
$^{2}ts_{b-is}$	1.876	1.885	1.886	1.879	2.124	1.511	-	1.066	-	1.329	-	117.6	-	125.7	160.3	158.7

Table S9. B3LYP-D2/B3LYP/wB97XD computed spin density values of the transition states of *Pathway b*.

B3LYP-D2	Fe	O1	H1	H2	O2	C1
			B3LYP-D2			
$^{4}ts_{b}$-1	2.853	0.267		0.008		-0.138
$^{2}ts_{b}$-1	1.462	-0.225		0.014		-0.157
$^{6}ts_{b}$-2_{hs}	3.981	0.133	-0.004		0.001	-0.097
$^{2}ts_{b}$-2_{is}	1.386	0.086	-0.006		-0.034	-0.437
			B3LYP			
$^{4}ts_{b}$-1	2.998	0.134		0.026		-0.287
$^{2}ts_{b}$-1	1.668	-0.374		0.035		-0.311
$^{6}ts_{b}$-2_{hs}	3.980	0.133	-0.004		0.001	-0.097
$^{2}ts_{b}$-2_{is}	2.672	0.059	-0.000		0.012	0.015
$^{2}ts_{b}$-2_{is}	1.386	0.086	-0.006		-0.034	-0.437
$^{2}ts_{b}$-2_{ls}	1.277	0.105	-0.004		-0.037	-0.391
			wB97XD			
$^{4}ts_{b}$-1	3.010	0.032		0.000		-0.177
$^{2}ts_{b}$-1	1.668	-0.374		0.035		-0.317
$^{6}ts_{b}$-2_{hs}	4.049	0.107	-0.000		0.004	-0.000
$^{2}ts_{b}$-2_{is}	2.734	0.074	0.004		0.006	0.004

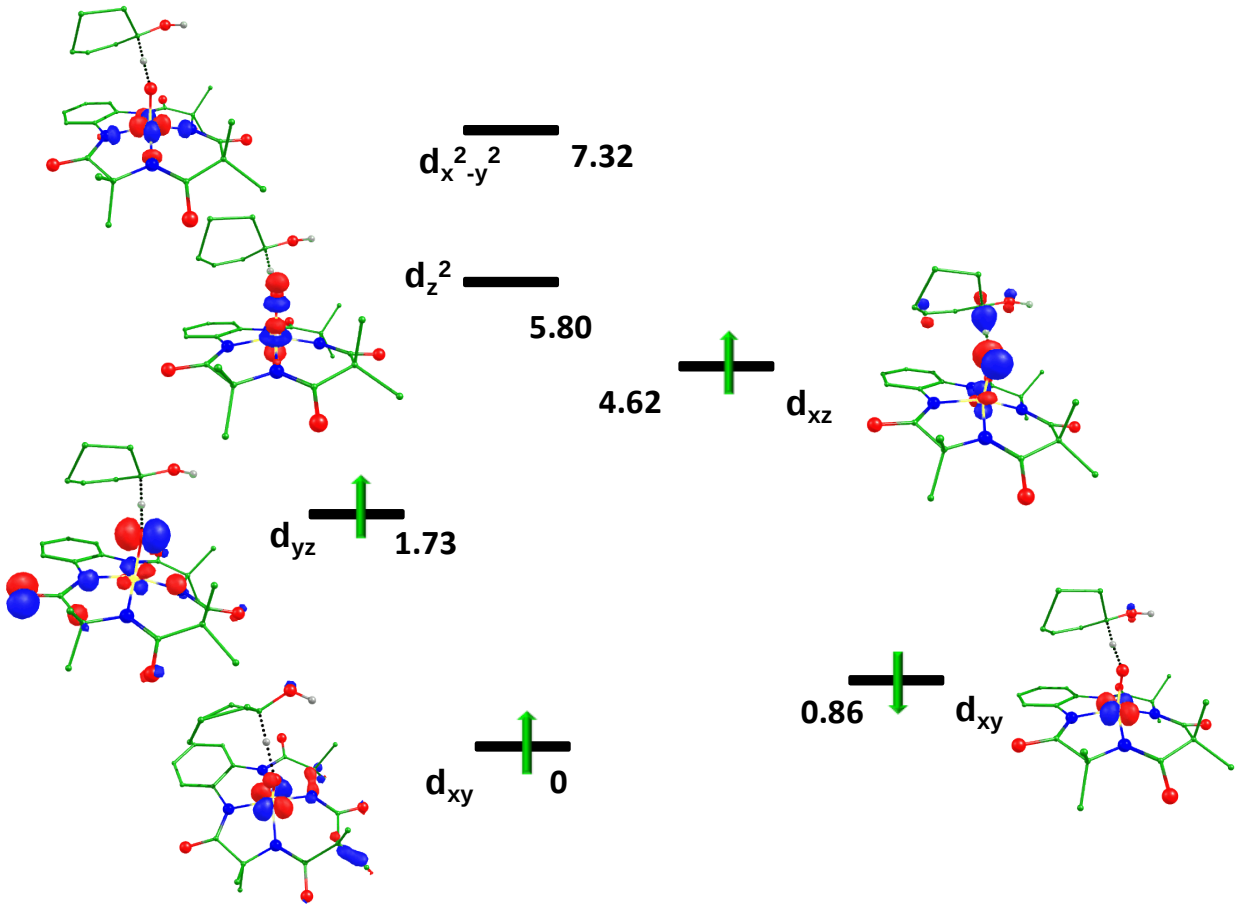

Fig. S8. Computed Eigen-value plot incorporating energies computed for d-based orbitals for alpha and beta spin corresponding to the ground state (^2ts_b-1) (energies are given in eV).

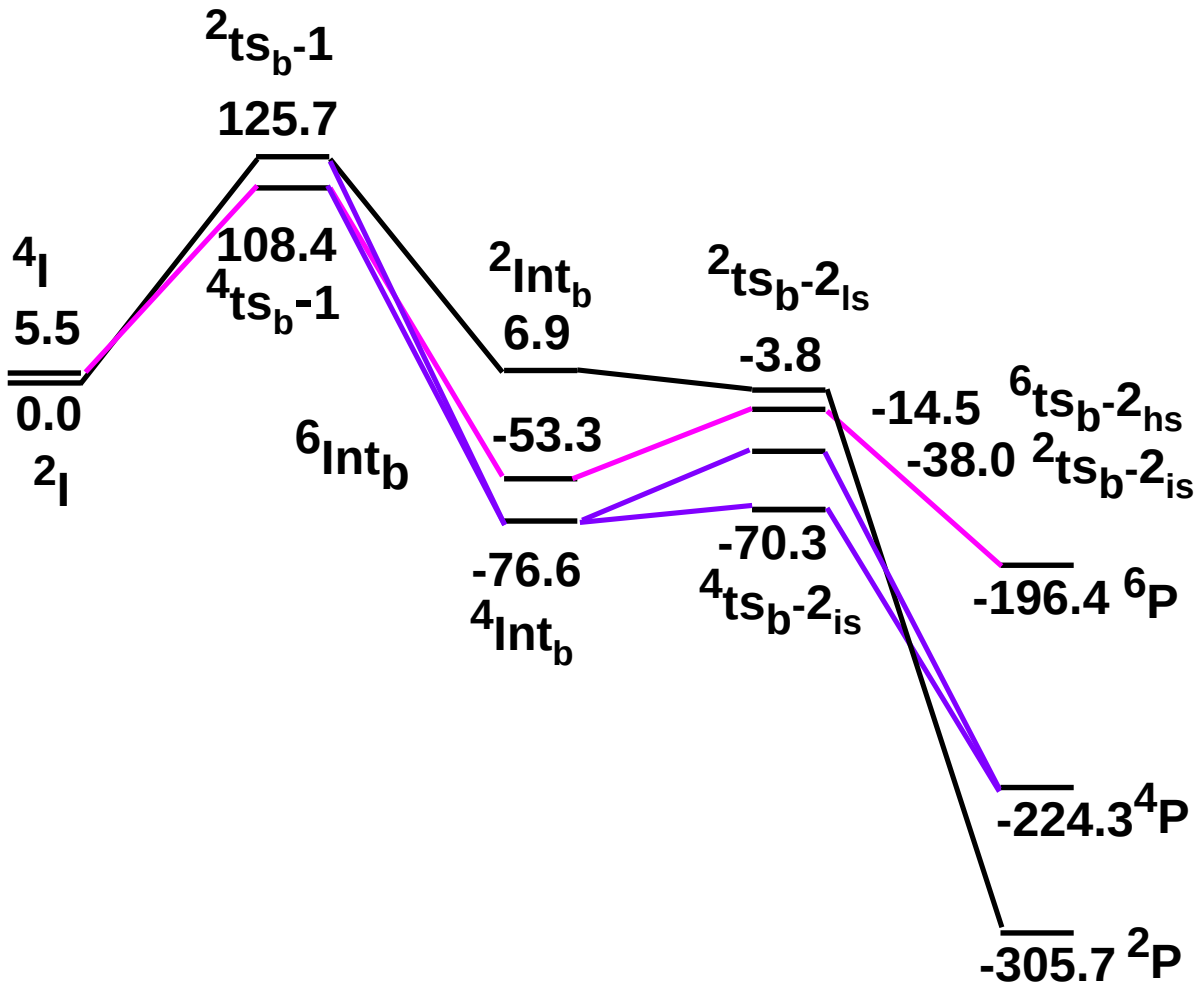

Fig. S9. B3LYP computed energy surface for the formation of cyclohex-2-enone from cyclohex-2-enol *via* C-H bond activation (***pathway b***) by Fe^{V}=O species (ΔG in $kJmol^{-1}$).

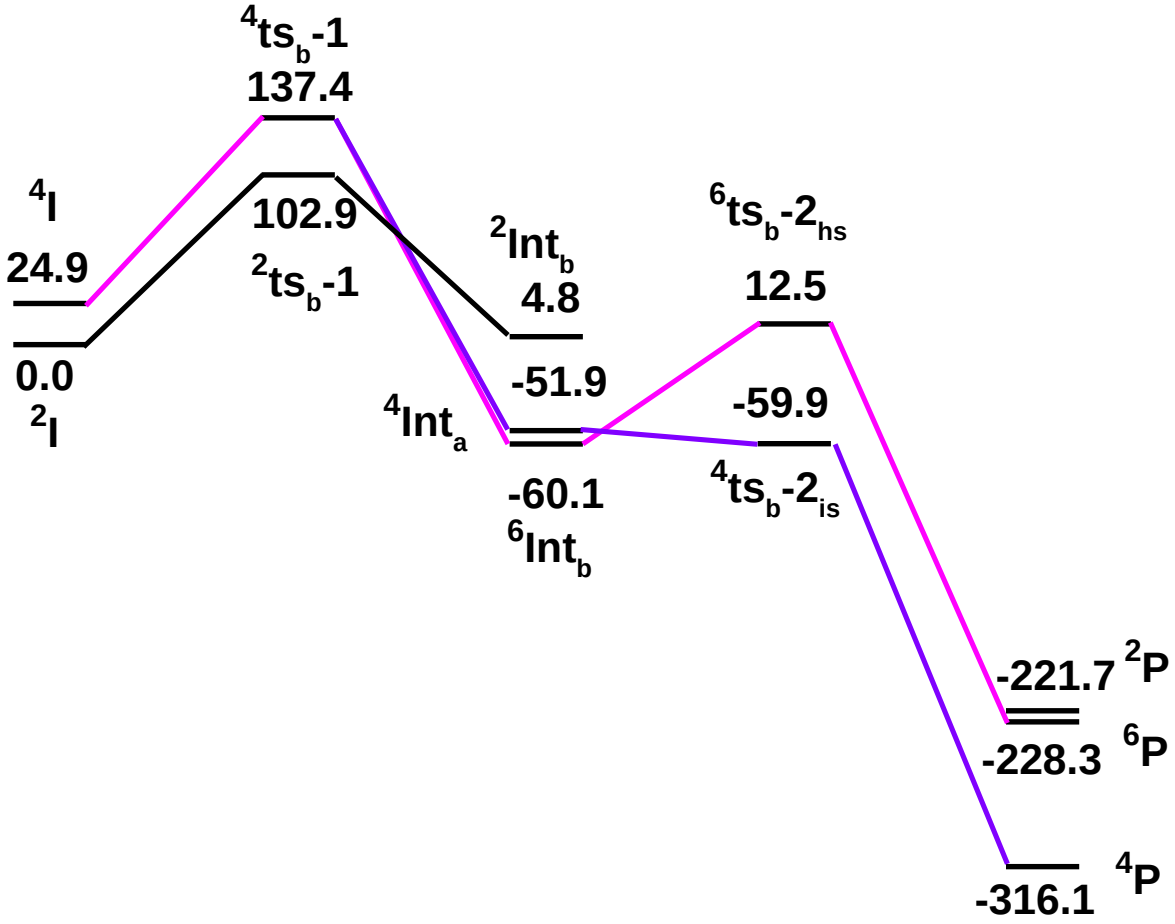

Fig. S10. wB97XD computed energy surface for the formation of cyclohex-2-enone from cyclohex-2-enol *via* C-H bond activation (***pathway b***) by Fe^{V}=O species (ΔG in $kJmol^{-1}$).

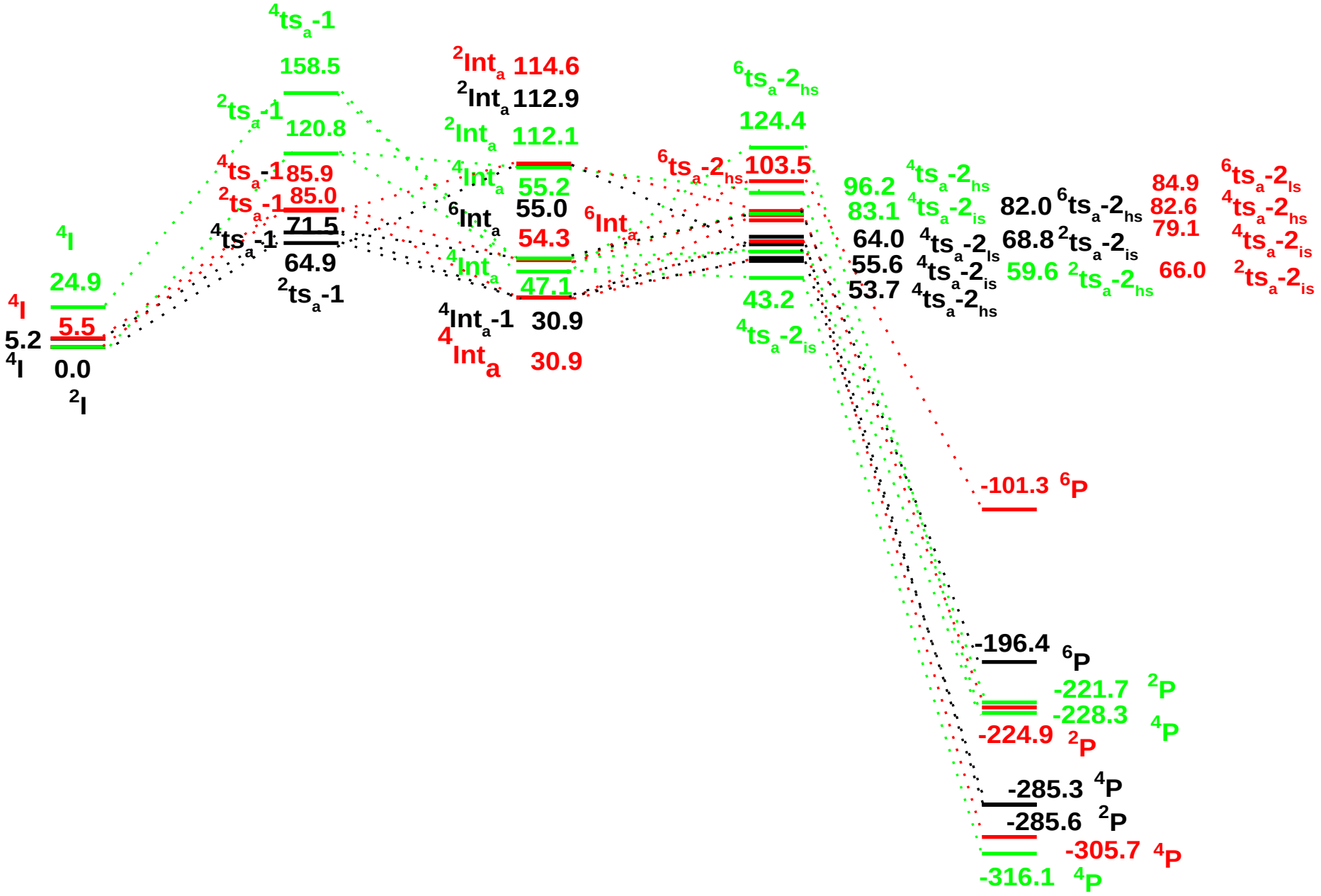

Fig. 11. B3LYP-D2 (black), B3LYP (red) and wB97XD (green) computed energy surface for the ground state of the ***pathway a*** (ΔG in kJmol^{-1}).

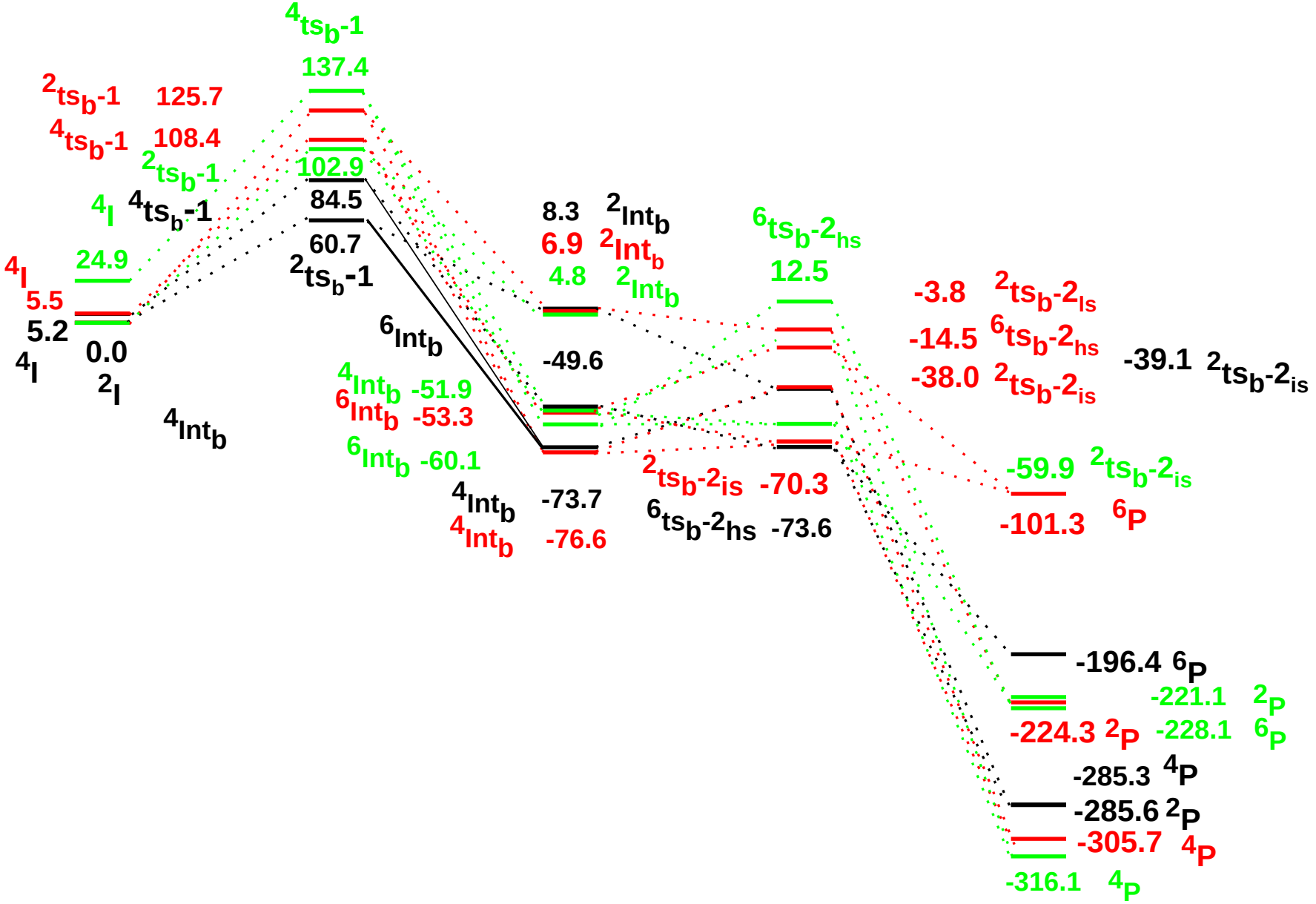

Fig. 12. B3LYP-D2 (black), B3LYP (red) and wB97XD (green) computed energy surface for the ground state of the ***pathway b*** (ΔG in kJmol^{-1}).

Full reference for reference number 27 of the main article

M. J. Frisch, G. W. Trucks, H. B. Schlegel, G. E. Scuseria, M. A. Robb, J. R. Cheeseman, G. Scalmani, V. Barone, B. Mennucci, G. A. Petersson, H. Nakatsuji, M. Caricato, X. Li, H. P. Hratchian, A. F. Izmaylov, J. Bloino, G. Zheng, J. L. Sonnenberg, M. Hada, M. Ehara, K. Toyota, R. Fukuda, J. Hasegawa, M. Ishida, T. Nakajima, Y. Honda, O. Kitao, H. Nakai, T. Vreven, J. A. Montgomery Jr., J. E. Peralta, F. Ogliaro, M. Bearpark, J. J. Heyd, E. Brothers, K. N. Kudin, V. N. Staroverov, R. Kobayashi, J. Normand, K. Raghavachari, A. Rendell, J. C. Burant, S. S. Iyengar, J. Tomasi, M. Cossi, N. Rega, J. M. Millam, M. Klene, J. E. Knox, J. B. Cross, V. Bakken, C. Adamo, J. Jaramillo, R. Gomperts, R. E. Stratmann, O. Yazyev, A. J. Austin, R. Cammi, C. Pomelli, J. W. Ochterski, R. L. Martin, K. Morokuma, V. G. Zakrzewski, G. A. Voth, P. Salvador, J. J. Dannenberg, S. Dapprich, A. D. Daniels, Ö. Farkas, J. B. Foresman, J. V. Ortiz, J. Cioslowski and D. J. Fox, GAUSSIAN 09 (Revision A.1), Gaussian, Inc., Wallingford, CT, 2009.

Reference

1. F. T. de Oliveira, A. Chanda, D. Banerjee, X. Shan, S. Mondal, L. Que Jr., E. L. Bominaar, E. Munck and T. J. Collins, *Science*, 2007, **315**, 835-838.